# Approximate Quantum Approaches to the Calculation of Resonances in Reactive and Nonreactive Scattering

JOEL M. BOWMAN[1], KI TUNG LEE[1,3], HUBERT ROMANOWSKI[1,4], and LAWRENCE B. HARDING[2]

[1]Department of Chemistry, Illinois Institute of Technology, Chicago, IL 60616
[2]Chemistry Division, Argonne National Laboratory, Argonne, IL 60439



**Reduced-dimensionality, quantum differential cross sections and partial wave cumulative reaction probabilities are presented for resonant and non-resonant scattering in the $H+H_2(v=0)$ reaction. The distorted wave Born approximation is tested against previous complex coordinate calculations of resonance energies and widths for a model van der Waals system. This approximation is subsequently used to obtain resonance energies and widths for the HCO radical using an approximate scattering path hamiltonian based on an *ab initio* potential energy surface. Several advantages of this hamiltonian for addition reactions are discussed.**

It is by now well established theoretically and experimentally that resonances are prominent features in non-reactive molecular systems. Although less evidence is available for reactive systems it is clear that resonances are also present for them. We have been investigating resonances in both kinds of systems and we present some of our recent results in this paper. Depending on the approach, resonances

[3]Current address: Department of Chemistry, University of Rochester, Rochester, NY.
[4]Permanent address: Institute of Chemistry, The Wroclaw University, 50-383 Wroclaw, Poland.

0097-6156/84/0263-0043$06.00/0

can be difficult or easy to obtain theoretically. They are difficult to locate in scattering calculations because their location is effectively unknown and must be uncovered by a search method. Direct, easy methods are those $L^2$ ones which locate the resonances and only the resonances. Of course the scattering methods give the most detailed information possible about the scattering at a resonance and indeed the two methods can be used in a complementary fashion. Both types of calculations scale exponentially with the number of coupled degrees of freedom and therefore they can quickly become computationally intractable. Thus, for both the scattering and direct methods we have been interested in reduced-dimensionality strategies to reduce the number of coupled degrees of freedom.

In the reduced-dimensionality space the dynamics is treated exactly, e.g., by the quantum coupled-channel approach. The remaining degrees of freedom are described in one of several approximate ways which will be reviewed below. The advantage of this approach is that it is feasible for systems of arbitrary complexity. In addition, it enables one to calculate cross sections, rate constants, etc. that are implicitly averaged over those degrees of freedom not explicitly treated dynamically, thus enabling a direct comparison to experiments which in most cases are not fully state-resolved. The degrees of freedom which are neither state-resolved experimentally nor treated dynamically will often be the same because they are usually the low-frequency motions such as rotation which are widely populated initially and finally in a collision. In the next section we shall review the elements of this theory for reactive systems with particular emphasis on resonances.

Following that we present calculations on resonances in a two-mathematical-dimensional (2MD) model for van der Waals systems. We will compare the complex eigenvalues obtained previously(1) by the complex coordinate method with those obtained from the distorted wave Born approximation (DWBA). Part of the motivation for making this comparison is to assess the accuracy of the DWBA before applying it to more realistic problems.

That is done in the penultimate section where we present some preliminary DWBA calculations of the resonances in the H+CO -> HCO addition reaction using a fit to an **ab initio** potential energy surface. A reduced-dimensionalty scattering space is derived based on a novel scattering path hamiltonian.

A summary and prognosis for further work are given in the final section.

## Model differential cross sections for $H+H_2(v=0)$

For the reactive systems we have studied the choice of a reduced-dimensionality space is obvious because the lowest-energy configura-

tion in all of these systems is the collinear one. This allows us to easily describe the reaction with standard Jacobi scattering coordinates, for which the kinetic energy operator is quite simple. With this approximation we have calculated quite accurate rotationally averaged and summed but vibrational state-to-state cross sections and rate constants for $H+H_2(v=0,1)$(2-4), $D+H_2(v=0,1)$(5), $O(^3P)+H_2(v=0,1)$ and $D_2(v=0,1)$(6,7). We have also given an expression for the differential cross section which is intended to be a simple model to predict the effect of resonances which are present in the reduced-dimensionality space on differential cross sections. This model has been applied to the $F+H_2$(8) and F+HD(9) reactions. The differential cross section for the vibrational state-to-state transition v to v' averaged over initial rotational states and summed over final ones is given by(8-10)

$$d\bar{\sigma}_{v->v'}(\theta)/d\Omega = 1/(4\bar{k}_v^2)\left|\sum_{J=0} (2J+1)S^{Jn\Omega}_{v->v'} d^J_{\Omega\Omega}(\theta)\right|^2 \qquad (1)$$

where

$$\bar{k}_v^2 = \sum_{j=0} (2j+1)k^2_{vj} \quad \text{and} \quad k^2_{vj} = 2\mu(E-E_v-E_j)/\hbar^2 \qquad (2)$$

E is the total energy and $E_v$ and $E_j$ are the vibrational and rotational energies of the reactant diatomic molecule. $d^J_{\Omega\Omega}(\theta)$ equals $D^J_{\Omega\Omega}(0,\theta,0)$, the rotation matrix and $\theta$ is the angle between the reactant and product arrangement channel body-fixed z-axes(11). $S^{Jn\Omega}_{v->v'}$ is the reduced-dimensionality partial wave scattering matrix which is obtained from approximate solutions to the three-dimensional Schroedinger equation, expressed in body-fixed coordinates(11-13). These solutions are based on the centrifugal sudden(14) and adiabatic approximation applied to the three-atom bending motion(10). For collinearly-favored reactions the adiabatic bending state, $|n\Omega\rangle$, is labeled by two quantum numbers, n and $\Omega$, where $\Omega$ is the z-component of the molecular angular momentum in the body-fixed frame (which also equals the z-component of the total angular momentum J in the body-fixed frame)(11). In the centrifugal sudden approximation $\Omega$ is a good quantum number, and for the adiabatic bending wavefunction n is restricted to the range $-\Omega \leq n \leq \Omega$ in steps of two(15). In terms of $S^{Jn\Omega}_{v->v'}$, the partial wave rotationally cumulative reaction probability is given by(10)

$$P^J_{v->v'} = \sum_{n\Omega} |S^{Jn\Omega}_{v->v'}|^2 \qquad (3)$$

where the summation is over the bending states. This probability is related to the physical ones by

$$P^J_{v->v'} = \sum_{j\Omega} \sum_{j'\Omega'} P^J_{vj\Omega->v'j'\Omega'} \qquad (4)$$

where $P^J_{vj\Omega->v'j'\Omega'}$ is the complete vibrational-rotational, state-to-state reaction probability.

The scattering matrix $S^{Jn\Omega}_{v->v'}$, is obtained from the asymptotic behavior of the scattering solutions to the following body-fixed Schroedinger equation(10)

$$\{-(\hbar^2/2\mu)(\partial^2/\partial R^2 + \partial^2/\partial r^2) + [J(J+1)-2\Omega^2]\hbar^2/(2\mu R^2)$$

$$+ V(r,R,\gamma=0) + \varepsilon_{n\Omega}(r,R) - E\} U^J_{n\Omega}(r,R) = 0 \qquad (5)$$

where R is the mass-scaled Delves radial distance of the atom A with respect to the center-of-mass of the reactant diatom BC and r is the mass-scaled diatom separation, $V(r,R,\gamma=0)$ is the collinear potential energy surface, $\varepsilon_{n\Omega}(r,R)$ is the ABC adiabatic bending eigenvalue which depends on r and R(10). The reduced mass $\mu$ is given by(11)

$$\mu = m_A m_B m_C/(m_A+m_B+m_C) \qquad (6)$$

Consider the particular case of the ground state bend, i.e., $n=\Omega=0$. We have introduced two approximations to Equation 5. within the spirit of transition state theory(2,3,10). The first one consists of replacing the centrifugal potential $J(J+1)\hbar^2/(2\mu R^2)$ by its value at the transition state, $E^{\ddagger}_J$, i.e., $J(J+1)\hbar^2/(2\mu R^{\ddagger 2})$, where $R^{\ddagger}$ is the value of R at the transition state. In this approximation $S^{J00}_{v->v'}$, is related to the scattering matrix corresponding to Equation 5. with no centrifugal potential, $S^{CEQB}_{v->v'}(E)$, by (10)

$$S^{J00}_{v->v'}(E) = (-1)^J S^{CEQB}_{v->v'}(E-E^{\ddagger}_J | n=\Omega=0) \qquad (7)$$

The corresponding CEQB probability is

$$P^J_{v->v'} = |S^{CEQB}_{v->v'}(E-E^{\ddagger}_J|n=\Omega=0)|^2 = P^{CEQB}_{v->v'}(E-E^{\ddagger}_J) \qquad (7a)$$

The notation CEQB stands for collinear exact quantum with an adiabatic treatment of the bending motion. The factor $(-1)^J$ accounts for a trivial difference in the asymptotic behavior of $U^J_{00}(r,R)$ and $U^{CEQB}_{00}(r,R)$, the CEQB wavefunction for the ground state bend, from which $S^{CEQB}_{v->v'}$, is obtained(10). The replacement of the centrifugal potential by an energy shift $E^{\ddagger}_J$ reduces the computational effort considerably.

Another and further approximation we have considered is to replace $\varepsilon_{00}(r,R)$ by $\varepsilon^{\ddagger}_{00}$, the value of the ground state bending energy at the transition state. In this further approximation $S^{J00}_{v->v'}$, is related to CEQ (collinear exact quantum) scattering matrix by

$$S^{J00}_{v->v'}(E) = (-1)^J S^{CEQ}_{v->v'}(E-E^{\ddagger}_J-\varepsilon^{\ddagger}_{00}) \qquad (8)$$

where $S^{CEQ}_{v->v'}$, is the scattering matrix corresponding to Equation 5. with no centrifugal potential and no adiabatic bending eigenvalue. In this case that equation looks exactly like the usual collinear Schroedinger equation.

We have focused on the ground state bending case for the following reason. As noted, Equation 1. represents a rotationally averaged and summed differential cross section. Specifically,

$$d\bar{\sigma}_{v->v'}(\Theta)/d\Omega = (1/\bar{k}^2_v) \sum_j (2j+1)k^2_{vj} d\sigma_{vj->v'j'}(\Theta)/d\Omega \qquad (9)$$

where $d\sigma_{vj->v'j'}(\Theta)/d\Omega$ is the usual degeneracy-averaged differential cross section. While we do not assume an adiabatic correlation

between bending and asymptotic free-rotor states, we do expect (assume) that the single term, n=Ω=0, in Equation 1. contains information mainly about the low-lying j and j' states in Equation 9. Based on this expectation we have restricted our previous calculations of differential cross sections (using the CEQ approximation to $S^{J00}_{v->v'}$) to the ground state bend(8,9). In this case Equation 1. can be written explicitly as

$$d\bar{\sigma}_{v->v'}(\Theta)/d\Omega = 1/(4\bar{k}_v^2) \left| \sum_{J=0} (2J+1) S^{J00}_{v->v'} P_J(\cos\Theta) \right|^2 \qquad (10)$$

where $P_J(\cos\Theta)$ is the Legendre polynomial of order J.

We have not yet implemented the fully adiabatic theory represented by Equation 5. That theory bears some resemblance to the bending-corrected rotating linear model (BCRLM)(16-18). In this model a partial wave hamiltonian is given by

$$H^{\ell} = -(\hbar^2/2\mu)(\partial^2/\partial u^2 + \partial^2/\partial w^2) + [\ell(\ell+1)+1]\hbar^2/2\mu Q^2 + V(u,w) + E_0^b(u) \qquad (11)$$

where $\ell$ is the orbital angular momentum, u is a reference reaction path coordinate, w is the coordinate transverse to u, and $E_0^b(u)$ is the ground state adiabatic bending energy evaluated on u, i.e., for w=0, and

$$Q^2 = R^2 + r^2 \qquad (12)$$

Scattering solutions to $(H^{\ell} - E)\psi^{\ell}(u,w)$ are obtained and the differential cross section is given by

$$\sigma^{BCRLM}_{v->v'}(\Theta) = (1/4k^2_{vj=0}) \left| \sum_{\ell=0} (2\ell+1) S^{\ell}_{v->v'} P_{\ell}(\cos\Theta) \right|^2 \qquad (13)$$

where $k^2_{vj=0}$ is given by Equation 2.

There are a number of differences between the BCRLM and the present adiabtic bending model. First, the total angular momentum J is used in Equation 5. whereas the orbital angular momentum $\ell$ appears in the BCRLM equations. Second, the centrifugal potentials containing these angular momenta are different, the one given in BCRLM does not vanish asymptotically, whereas the one in Equation 5. does. Another difference is the use of $k^2_{vj=0}$ in Equation 13. instead of the average squared wavevector $\bar{k}^2_v$. This last difference arises because the differential cross section we have given is explicitly a rotationally summed and averaged quantity whereas the exact identity of the BCRLM differential cross section is still ambiguous(17).

We applied Equations 3., 7a. and 10. to a study of cumulative reaction probabilities and differential cross sections for $H+H_2(v=0) -> H_2(v'=0)+H$ using the PK2 potential energy surface(19) in the total energy range 0.6 to 0.95 eV. The upper end of this range contains part of a broad resonance which is centered at 0.965 eV, in good agreement with the accurate quantum calculations for the J=0 partial wave of Schatz and Kuppermann(20), who found the resonance centered at 0.973 eV.





Truhlar, Donald G.;
ACS Symposium Series; American Chemical Society: Washington, DC, 1984.

In Figure 1 we have plotted the partial wave cumulative reaction probabilities $P^J_{0->0}$ versus J and the corresponding differential cross sections for total energies of 0.6 and 0.7 eV. Both sets of probabilities display a monotonic decrease with J and the differential cross sections both decline smoothly from $\theta$ equal to 180°, in qualitative agreement with the accurate quantum results of Schatz and Kuppermann(11). Above 0.7 eV there are no accurate quantum differential cross sections for this reaction with which to compare the present calculations and so the results in Figure 2 should be regarded cautiously. There the partial wave cumulative reaction probabilities and differential cross sections are given for total energies of 0.8, 0.85, and 0.95 eV. As seen the $P^J_{0->0}$ show a flatter dependence on J for E equal to 0.8 and 0.85 eV and distinct structure at 0.95 eV. This latter behavior is quite interesting in that it shows a maximum at non-zero J. This is simply due to the resonance in the CEQB reaction probability $P^{CEQB}_{0->0}$ manifesting itself in the partial wave reaction probability according to Equation 7a. The minimum in the CEQB resonance occurs at a slightly higher energy than 0.95 eV, as already noted, however, the behavior of $P^{CEQB}_{0->0}$ is such that as E decreases somewhat from 0.95 eV the probability increases until E decreases sufficiently so that $P^{CEQB}_{0->0}$ declines to zero. It is interesting that the differential cross sections at 0.8, 0.85, and 0.95 eV all show structure, even though the partial wave cumulative reaction probabilities do not show obvious structure at the two lower energies. This suggests that there is no simple correlation between structure in the differential cross section and structure in the partial wave reaction probabilities. However, it does seem reasonable that if $P^{CEQB}_{0->0}$ does show structure then so will the corresponding differential cross section.

The results presented here are in support of earlier studies which have correlated structure in the partial wave reaction probabilities and structure in the differential cross sections. Especially noteworthy among these earlier studies are the ones of Redmon and Wyatt(21) who first suggested this correlation based on their $j_z$-conserving quantum calculations of the $F+H_2$ -> HF+H reaction. We applied the CEQ version of the reduced dimensionality method to a study of that reaction(8) as well as the F+HD -> HF+D, DF+H reactions(9) and found similar correlations. More recently the BCRLM was used in an extensive study of differential cross sections in the $F+H_2$, $D_2$, and HD reactions(17). (Also, see the paper by Hayes and Walker in this volume.)

A scattering calculation gives the most complete description of resonances in reactive and non-reactive systems. However, if the resonances are the major features of interest a more direct approach to obtain them is desirable. A number of such aproaches exist and are reviewed in this volume and in the following sections of this paper. These have been applied mainly to non-reactive systems, however, they are beginning to be used in reactive systems. Thus far they have been applied to collinear reactive systems where their accuracy is being tested. The status of these calculations is discussed in a paper by Garrett et al. in this volume.

Of these direct approaches the complex coordinate method is the most rigorous one. In principle it yields the exact energies of the poles of the scattering matrix, which, ignoring the background contribution to the scattering, gives the resonance position and width.

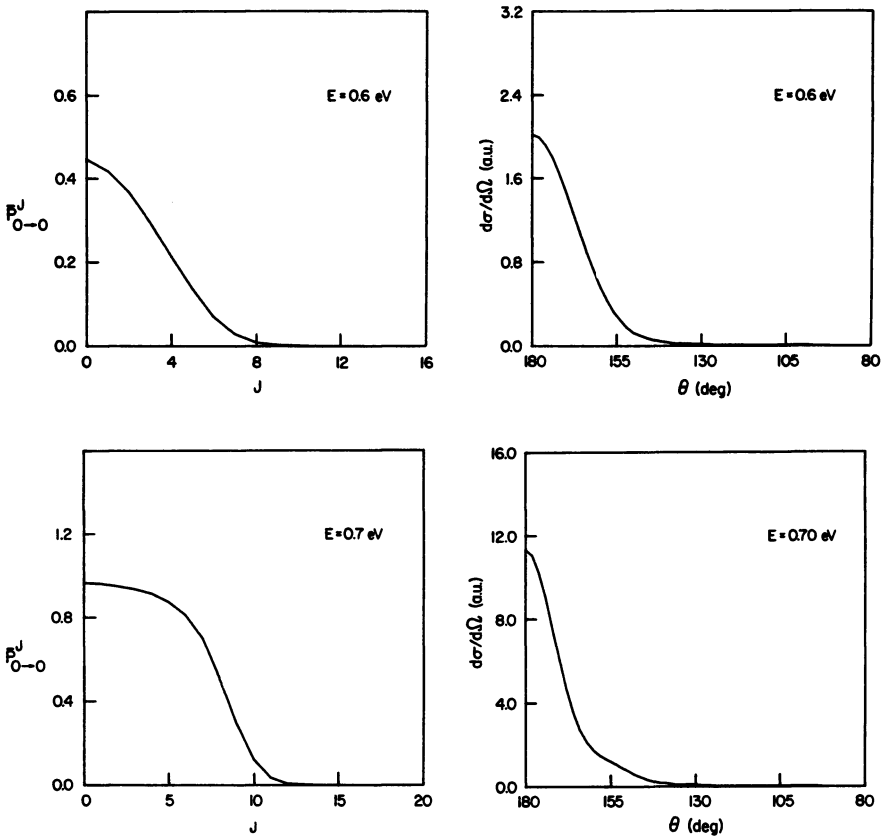


**Figure. 1 CEQB cumulative partial wave reaction probabilities versus total angular momentum for H+$H_2$(v=0) -> $H_2$(v'=0)+H and corresponding differential cross section for total energies of 0.6 and 0.7 eV.**

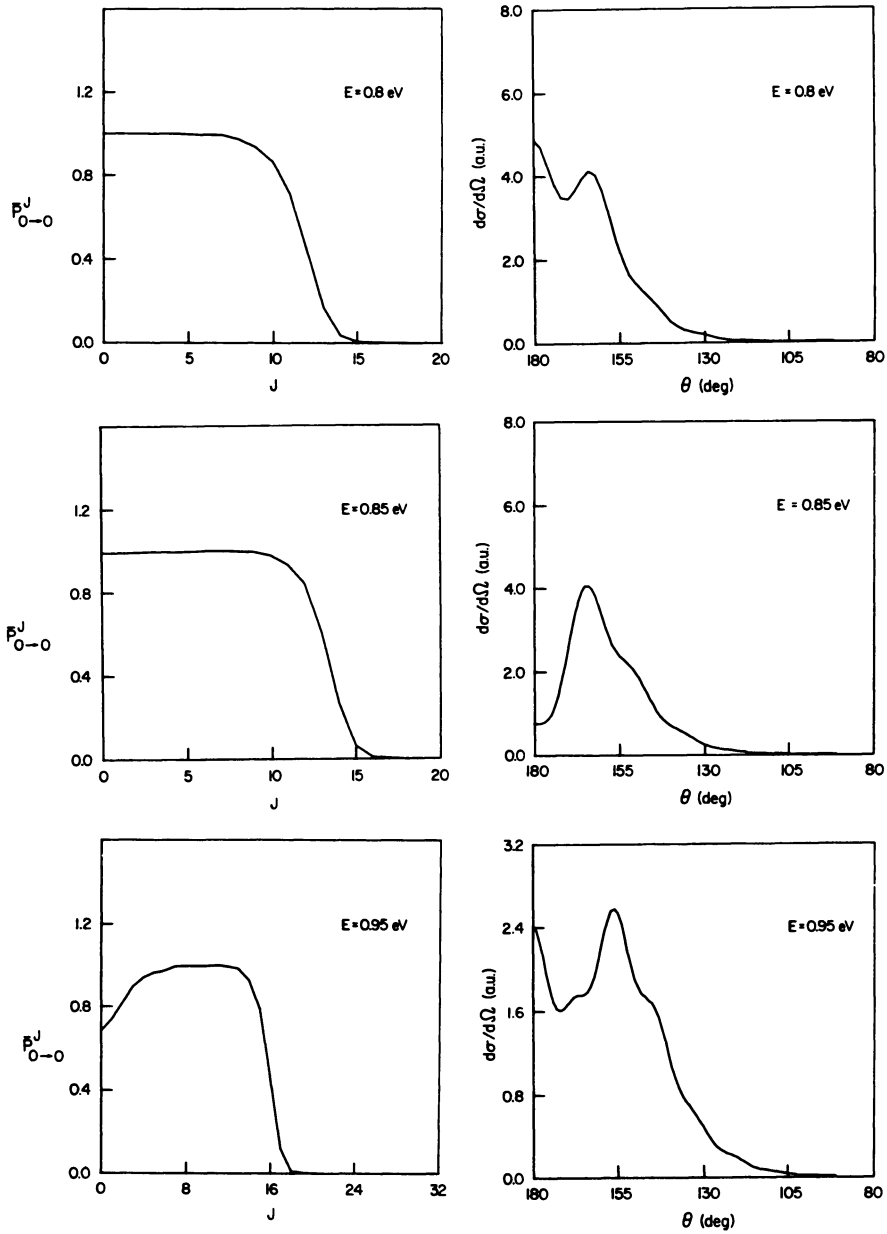


**Figure. 2 Same as Fig. 1 but for total energies just below the center energy of the resonance, 0.965 eV.**

There are many other approaches to obtain resonance energies and widths, many are reviewed in this volume. One that we consider in the next two sections is the distorted wave Born approximation (DWBA). In the following section the DWBA is tested against accurate complex coordinate calculations reported previously for a collinear model van der Waals system(1). The DWBA is then used to obtain the resonance energies and widths for the HCO radical. A scattering path hamiltonian is developed for that system and a 2MD approximation to it is given for the J=0 state.

## Distorted wave Born and complex coordinate resonances for a model van der Waals system.

The complex coordinate method was applied recently by Christoffel and Bowman(1) to a model collinear hamiltonian used earlier by Eastes and Marcus(22) in quantum and semiclassical studies of the resonances in that system. The hamiltonian is ($\hbar$=1)

$$H = -1/m(\partial^2/\partial x^2 + \partial^2/\partial y^2) + y^2$$

$$+ D\{\exp[-2\alpha(x-y)]-2\exp[-\alpha(x-y)]\} \qquad (14)$$

where the energy is in units of the zero-point energy of the harmonic oscillator (y-mode), m = 0.2, D = 1.5, and $\alpha$ = 0.1. This hamiltonian describes a harmonic oscillator the end atom of which interacts with a third atom by a Morse potential. This model has served as a paradigm in many quantum scattering studies(22-27). It is also a suitable model for linear atom-diatom van der Waals complexes and has been adopted for that purpose in a series of papers by Beswick and Jortner(28). For this hamiltonian the DWBA provides analytical expressions for the resonance widths, as shown by Beswick and Jortner(29) and much earlier by Rosen(30). A very simple picture of the (Feshbach) resonances is given by partitioning H as

$$H = H_o + V_c(x,y) \qquad (15)$$

where $H_o$ is given by Equation 14. with y equal to zero in the Morse potential and therefore

$$V_c(x,y) = D\{1-\exp[\alpha(x-y)]\}^2 - D\{1-\exp(-\alpha x)\}^2 \qquad (16)$$

Those zero-order bound state eigenfunctions $\phi_v(y)\chi_m(x)$ which are energetically degenerate with continuum ones $\phi_{v'}(y)\chi_\varepsilon(x)$ are the resonance states, where $\phi_v(y)$ is a harmonic oscillator eigenfunction and $\chi_m(x)$ and $\chi_\varepsilon(x)$ are bound and energy-normalized continuum Morse oscillator eigenfunctions, respectively. For the system parameters chosen all zero-order bound states with v>0 are resonance states. This is because the harmonic oscillator quantized energy, 2v+1, is greater than D for v>0. In the DWBA the width of a resonance is given by(30)

$$\Gamma_{vm->v'\varepsilon} = 2\pi|\langle v'\varepsilon|V_c|vm\rangle|^2 \qquad (17)$$

The matrix element in Equation 17. can be evaluated analytically(29) and of course numerically. We did both to test the numerical method, based on a Cooley-Numerov integrator(31,32) which was used in later calculations.

The widths $\Gamma_{vm->v'\varepsilon}$ were calculated for v=1,2, and 3 and numerous values of m (there are ten bound states in the Morse potential for m=0.2) and for v'=v-1. The widths for v' less than v-1 are much smaller than the single quantum changes ones. The widths $F_{vm->v'\varepsilon}$ are related to the imaginary part of the complex energy pole of the scattering matrix by

$$\Gamma_{vm->v'\varepsilon} = -2\mathrm{Im}(E_{m,v}) \qquad (18)$$

The DWBA and available complex coordinate results for $-\mathrm{Im}(E_{m,v})$ are given in Figure 3. The zero-order resonance energies are given by

$$\mathrm{Re}(E_{m,v}) = 2v+1 + E_m \qquad (19)$$

where $E_m$ are the bound state Morse oscillator energies. The results naturally group into series for a given v in which m increases. Each group is bounded above in energy by 2v+1 because the last bound Morse level is close to but less than zero. There is good agreement between the complex coordinate and DWBA results, the latter are roughly 30% smaller than the accurate results. A striking mode specificity is seen in these results; clearly energy in the dissociative Morse degrees of freedom is more effective in the dissociation than energy in the harmonic degree of freedom. This is not a surprising result for such a weakly coupled system.

These results confirm and complement the earlier work of Beswick and Jortner who compared DWBA widths with those from collinear coupled-channel scattering calculations(33) where, as here, good agreement was observed. In the next section the DWBA widths are calculated for the chemically bonded HCO radical to give H+CO. Based on the present comparisons with exact results we are optimistic that the DWBA will provide realistic widths for this system.

## Resonances in the HCO system using an ab initio potential

The HCO potential surface was generated with Hartree-Fock plus all single and double excitation, configuration interaction calculations to which the Davidson correction(34,35) for quadruple excitations was added. The basis set employed was the standard polarized valence double zeta basis set of Dunning and Hay(36). These calculations lead to structures and energies, shown in Table I., similar to those obtained by Dunning(37). For the dynamical calculations presented here it is necessary to have global information on the surface in addition to the properties of the stationary points. This was obtained by carrying out **ab initio** calculations at approximately 2000 geometries. The energies from these calculations were fit, in localized regions, to Taylor series polynomials of the Simons-Parr-Finlan form(38,39). These analytic representations of local regions of the potential surface were then connected by hyperbolic tangent switching functions to give an analytic representation of the global surface having the same stationary point properties as the **ab initio** surface (Table I.).

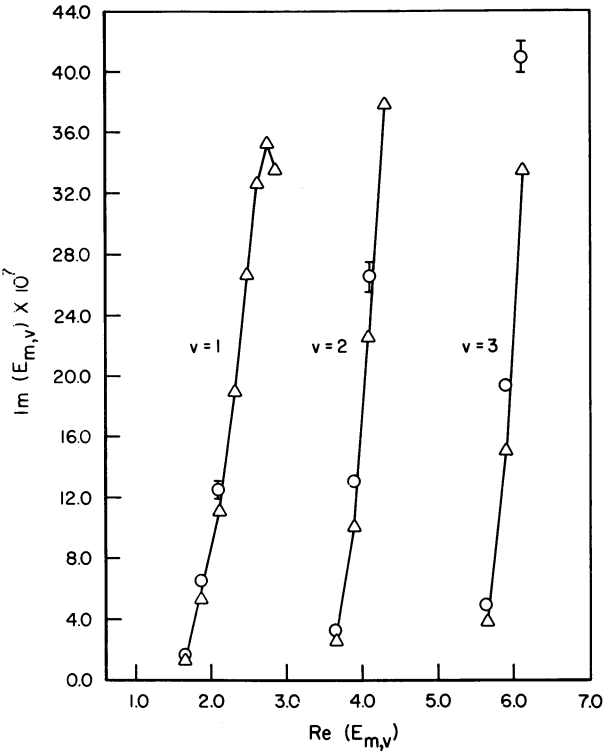


**Figure. 3 Comparison of previous complex-coordinate (O) (ref. 1) and present distorted wave Born (Δ) resonance half-widths and energies for a model van der Waals system. The half-widths are given by $-Im(E_{m,v})$ and the energies by $Re(E_{m,v})$.**

The ab initio calculations used here lead to a barrier height of 5.8 kcal/mol, while the observed activation energy for this reaction is reported to be approximately 2 kcal/mol(40), implying an error in the calculated barrier height of approximately 4 kcal/mol. Similarly, the ab initio calculations predict the addition of hydrogen to carbon monoxide to be 18.1 kcal/mol exothermic, while the best experimental estimate(41) of this energy difference is approximately 1 kcal/mol higher. To correct for these deficiencies in the calculated surface an empirical correction of the form,

$$E_{CORR} = (E_C/R_CH + E_O/R_{OH})/(1/R_{CH} + 1/R_{OH}) \quad (20)$$

was added to the ab initio potential energy surface, where $R_{CH}$ is the distance from the hydrogen to the carbon, $R_{OH}$ is the distance from the hydrogen to the oxygen, and where

$$E_C = A_C/\{\exp[B_C(R_{CH}-R^o_{CH})] + \exp[-C_C(R_{CH}-R^o_{CH})] + D_C\} \quad (21)$$

$$E_O = A_O/\{\exp[B_O(R_{OH}-R^o_{OH})] + \exp[-C_O(R_{OH}-R^o_{OH})] + D_O\}. \quad (22)$$

The parameters, A, B, C, D, $R^o_{CH}$ and $R^o_{OH}$ were chosen to match the experimental barrier height, reaction exothermicity, and CH stretching frequency of the formyl radical. Other characteristics of the surface are changed only slightly by this adjustment. The geometries, frequencies, and energies of the stationary points on this adjusted surface are also shown in Table I.

Table I. Calculated SDQ-CI structures and energies for the addition of atomic hydrogen to carbon monoxide. Values in parenthesis are from the adjusted surface (see text).

| | H + CO | H - CO | HCO |
|---|---|---|---|
| Geometries | | | |
| $R_{CO}$ | 2.173 (2.173) | 2.193 (2.181) | 2.259 (2.259) |
| $R_{CH}$ | - | 3.431 (3.495) | 2.116 (2.124) |
| ∠HCO(deg) | - | 119.0 (117.2) | 124.5 (124.2) |
| Harmonic frequencies ($cm^{-1}$) | | | |
| $\omega_1$ | 2173 (2173) | 1963 (2120) | 2815 (2748) |
| $\omega_2$ | - | 400 (400) | 1903 (1905) |
| $\omega_3$ | - | 1095i (589i) | 1156 (1145) |
| Total energies (hartree) | -113.54392 | -113.53472 | -113.57284 |
| Relative energies | 0.0 (0.0) | 5.8 (1.6) | -18.1 (-19.4) |

An equipotential contour plot of the potential surface is given in Figure 4 for a fixed $R_{CO}$ distance of 2.25 $a_o$, its value at the HCO minimum. The steepest descent paths (in mass-weighted cartesian coordinates) to the HCO minimum are shown from the primary, low-energy HCO saddle point and from a secondary, higher-energy saddle point for the collinear HCO configuration. Note that $R_{CO}$ does vary along these paths, although its value was fixed for the potential surface contour, as noted. Several features of this reaction path are noteworthy. First, $R_{CO}$ does not change very much along them. For example $R_{CO}$ changes by only +0.078 $a_o$ from its value at the primary energy saddle point to the minimum. Second, that branch of the path is nearly linear, except in the vicinity of the minimum. These facts suggest the following scattering scenario. The reactants approach along the reaction path initially, however, due to the presence of the HCO minimum and the rather weak coupling the H atom picks up kinetic energy rapidly and tends to follow a straight-line (diabatic) path into the hard-wall region of the potential, where it may undergo a resonant transition down into a bound state of the well while temporarily exciting the CO-stretch. For these reasons, we have adopted another path which we term a scattering path. This is a straight-line path connecting the low energy saddle point with the minimum and for a constant value of $R_{CO}$ given by its value at that saddle point, $R^{\ddagger}_{CO}$. The distance along this path is denoted t, the orthogonal transverse coordinate is u, and $R_{CO}$ is unchanged. For simplicity we shall make the following changes in notation, $R=R_{H,CO}$ and $r=R_{CO}$. Also, we shall replace $\gamma$ by the distance $r^{\ddagger}\gamma$. Thus, the transformation between the coordinates $(r^{\ddagger}\gamma,R)$ and (u,t) is given by

$$\begin{bmatrix} R-R^{\ddagger} \\ r^{\ddagger}(\gamma - \gamma^{\ddagger}) \end{bmatrix} = \begin{bmatrix} \cos\theta & -\sin\theta \\ \sin\theta & \cos\theta \end{bmatrix} \begin{bmatrix} t \\ u \end{bmatrix} \tag{23}$$

where

$$\tan\theta = r^{\ddagger}(\gamma^{\ddagger} - \gamma_o)/(R^{\ddagger} - R_o) \tag{24}$$

where $\gamma_o$ and $R_o$ are the values of $\gamma$ and R at the HCO minimum.

To obtain the scattering path hamiltonian we would begin with the general body-fixed hamiltonian in the variables $(R,\gamma,r)$(13) and simply re-express it in terms of the variables (t,u,r) using the above transformation. For simplicity we consider the zero partial wave, J=0, and we obtain

$$H = \frac{-\hbar^2}{2\mu_{H,CO}}\frac{\partial^2}{\partial R^2} \quad \frac{-\hbar^2}{2\mu_{CO}}\frac{\partial^2}{\partial r^2} \quad \frac{-\hbar^2}{2I(r,R)}\left(\frac{\partial^2}{\partial\gamma^2} + \cot\gamma\frac{\partial}{\partial\gamma}\right) + V(R,r,\gamma), \tag{25}$$

where

$$I^{-1}(R,r) = (\mu_{H,CO}R^2)^{-1} + (\mu_{CO}r^2)^{-1} \tag{26}$$

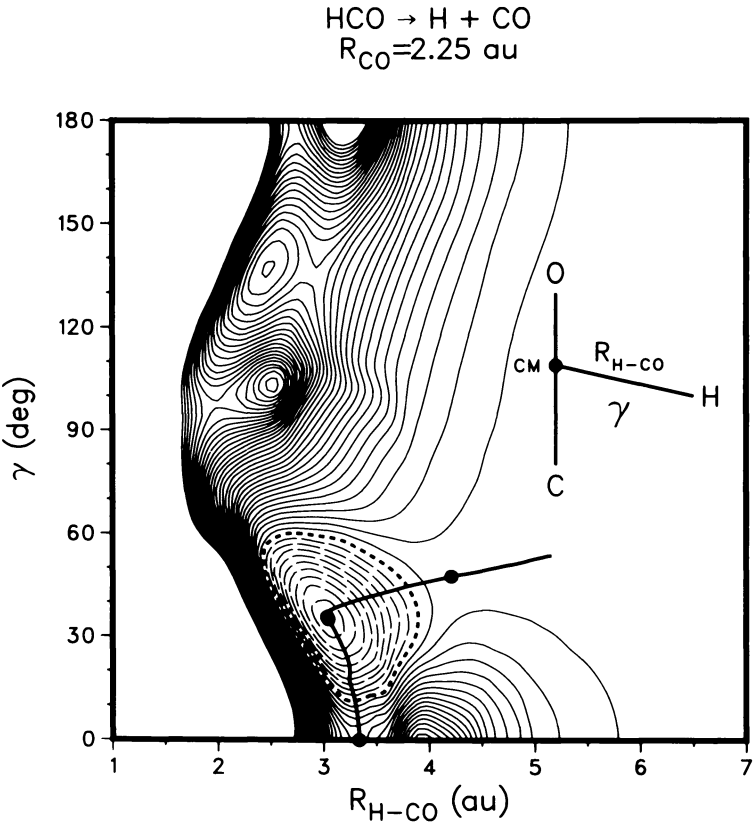


**Figure. 4 Equipotential energy contours obtained from ab initio calculations for the HCO system for $R_{CO}$ fixed at its value in HCO. The zero-energy contour is given by the thick dashed line, negative and positive energy contours are given by thin dashed and solid lines, respectively. The energy difference between adjacent contour lines is 2 kcal/mole. The paths shown are the paths of steepest descent in mass-weighted Cartesian coordinates (along which $R_{CO}$ varies) from the primary low energy saddle point to the HCO minimum and then to the secondary high energy collinear saddle point.**

The Schroedinger equation is

$$(H-E)\,\psi(R,r,\gamma) = 0 \tag{27}$$

where

$$\psi(R,r,\gamma) = (rR)\,\Psi(R,r,\gamma) \tag{28}$$

and $\Psi(R,r,\gamma)$ is the eigenfunction of the body-fixed hamiltonian containing first derivative terms in R and r. Before rewriting Equation 27. in terms of the new variable (t,u,r) we approximate $I^{-1}(R,r)$ by replacing r by $r^{\ddagger}$. This is justified in the present case because as noted r does not change very much from $r^{\ddagger}$ along the reaction path and is assumed to be constant along the scattering path. Thus, we replace $I^{-1}$ by the approximation

$$I^{-1} = [(1/\mu_{H,CO})(r^{\ddagger}/R)^2 + 1/\mu_{CO}]/r^{\ddagger 2} \tag{29}$$

and rewrite Equation 25. as

$$H = \frac{-\hbar^2}{2\mu_{H,CO}}\frac{\partial^2}{\partial R^2} \frac{-\hbar^2}{2\mu_{CO}}\frac{\partial^2}{\partial r^2} \frac{-\hbar^2}{2\mu(R)}\left(\frac{1}{r^{\ddagger 2}}\frac{\partial^2}{\partial\gamma^2} + \cot\gamma\frac{\partial}{\partial\gamma}\right) + V(R,r,\gamma) \tag{30}$$

where

$$1/\mu(R) = 1/\mu_{CO} + 1/[\mu_{H,CO}(R/r^{\ddagger 2})] \tag{31}$$

The transformation of Equation 30. to the (t,u,r) coordinate system is straightforward, with the following result.

$$H = \frac{-\hbar^2}{2}\left(\frac{\cos^2\theta}{\mu_{H,CO}} + \frac{\sin^2\theta}{\mu(R)}\right)\frac{\partial^2}{\partial t^2} \frac{-\hbar^2}{2}\left(\frac{\cos^2\theta}{\mu(R)} + \frac{\sin^2\theta}{\mu_{H,CO}}\right)\frac{\partial^2}{\partial u^2} \frac{-\hbar^2}{2\mu_{CO}}\frac{\partial^2}{\partial r^2}$$
$$+ T(u,\partial/\partial u,t,\partial/\partial t) + V(t,r,u) \tag{32}$$

where

$$T(u,\partial/\partial u,t,\partial/\partial t) = -[\hbar^2/2\mu(R)](\cot\gamma/r^{\ddagger})(\sin\theta\partial/\partial t + \cos\theta\partial/\partial u) \tag{33}$$

One advantage of this scattering path hamiltonian is that the potential can be written as

$$V(t,r,u) = V_o(t) + V'(r,u,t) \tag{34}$$

where $V_o(t)$ is the potential along the scattering path. This will be shown and discussed below. Another advantage of Equation 32. is that reduced dimensionality quantum approaches to the calculation of the inelastic scattering can be easily implemented. Our focus here is on the resonance energies and widths of the HCO complex and in particular those which are due to temporary excitation of the CO stretch. Thus, we shall simply ignore the u-motion hereafter. (Other approximate, e.g. adiabatic, treatments of it could be considered.) In addition, $\cos^2\theta = 0.87$, $\sin^2\theta = 0.13$ and $\mu(R)$ is roughly several times $\mu_{H,CO}$ for values of R in the vicinity of the HCO minimum. Thus, the term $\sin^2\theta/\mu(R)$ is roughly an order of magnitude smaller than $\cos^2\theta/\mu_{H,CO}$, and so we shall ignore it.

This gives

$$h = \frac{-\hbar^2}{2\mu_{H,CO}/\cos^2\theta}\frac{\partial^2}{\partial t^2} \frac{-\hbar^2}{2\mu_{CO}}\frac{\partial^2}{\partial r^2} + V_o(t) + V'(r,t) \qquad (35)$$

for the reduced-dimensionality hamiltonian. This hamiltonian was used in distorted wave Born approximation calculations of resonances, as described in the previous section and the results are given below.

DWBA calculation of resonances. The variation of $R_{CO}$, $R_{H,CO}$, $\gamma$, and the potential with t is shown in Figure 5 for the straight-line scattering path and the portion of the reaction path shown in Figure 4 from the primary saddle point to the HCO minimum. There is good agreement between the paths, however, when considering the potential V'(r,t) (recall r=$R_{CO}$) there are important differences. For the scattering path

$$V'(r,t) = a(t)(r-r^*) + b(t)(r-r^*)^2 + \ldots \qquad (36)$$

whereas for the reaction path the normal modes transverse to it (one of which is close to being the CO stretch) do not contain a linear term in a Taylor series representation of the potential(42,43). This difference between the form of the potential for the mode transverse to the reference scattering or reaction path has important consequences for the nature of resonance states, as discussed below.

Distorted wave Born approximation resonance energies and widths were calculated numerically using Equation 17. for the reduced-dimensionality hamiltonian given by Equation 35. and employing Equation 36. for V'(r,t) up to second order. The coefficients a(t) and b(t) were determined numerically from the ab initio potential surface. Zero-order wavefunctions $\phi_v(r)$, $\chi_m(t)$ and $\chi_\varepsilon(t)$ were determined as follows. The $\phi_v(r)$ are harmonic oscillator functions for CO with a frequency of 2172.6 $cm^{-1}$, as determined from the ab initio surface and $\chi_m(t)$ and $\chi_\varepsilon(t)$ are the bound and continuum eigenfunctions of the zero-order hamiltonian

$$h_m = \frac{-\hbar^2}{2\mu_{H,CO}/\cos^2\theta}\frac{d^2}{dt^2} + V_o(t) \qquad (37)$$

They were determined numerically by the Cooley-Numerov method(31,32), with a spline representation of $V_o(t)$. The $V_o(t)$ potential supports three bound states.

The general expression for the DWBA width (cf. Equation 17.) can be written as

$$\Gamma_{vm->v'\varepsilon} = 2\pi|\langle v'|r-r^*|v\rangle\langle\varepsilon|a(t)|m\rangle+\langle v'|(r-r^*)^2|v\rangle\langle\varepsilon|b(t)|m\rangle|^2 \qquad (38)$$

Thus, only $\Delta v = -1$ and $\Delta v = -2$ transitions can occur, the first term is responsible for the former and the second term is responsible for the latter. (Strictly, because $r^*$ is not quite equal to the equilibrium CO distance, the second term can also give rise to $\Delta v = -1$ transitions, however, those are negligible compared to those due to

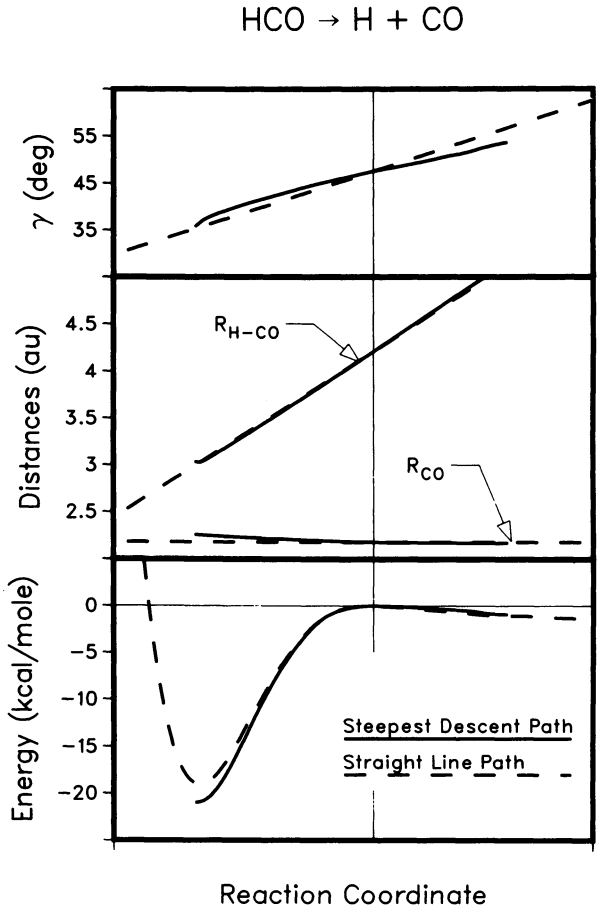


**Figure. 5 The variation of γ, $R_{H-CO}$, $R_{CO}$ and the potential energy along the steepest descent (solid line) and straight line (dashed line) paths described in the text. Only the portion of the former path from the primary saddle point to the HCO minimum is shown.**

the first term because the above two distances differ by only 0.008 $a_o$.)

Because only three zero-order bound states are supported by $V_o(t)$ it is possible to classify the widths into three categories. For the $\Delta v = -1$ transitions only the highest bound state of $V_o(t)$ is metastable. That is, the energy released in the $\Delta v = -1$ transition is only sufficient to cause this highest bound state to make the transition to the continuum. For $\Delta v = -2$ transitions the two excited states of $V_o(t)$ are metastable. The zero-order resonance energies and DWBA widths are given in Table II. for a number of states and the numerical expressions used to evaluate them are given as footnotes there. As seen the $\Delta v = -1$ widths are considerably larger than the $\Delta v = -2$ ones. The latter ones are on the order of those found for $\Delta v = -1$ widths in van der Waals systems(28). The present $\Delta v = -1$ widths are therefore considerably larger than those seen in van der Waals systems. This is not unexpected because the HCO complex is clearly more strongly coupled than a van der Waals system. It should be noted that at total energies greater than 1.5 eV resonances due to the HOC complex also occur and these are discussed in the paper by Geiger et al.(44) in this volume.

Table II. Distorted wave Born approximation resonance energies and widths for two-mode HCO (in eV).

| v | [a] $E_{v,m=2}$ | [b] $\Gamma_{\Delta v=-1}$ | [c] $\Gamma_{\Delta v=-2}$ | [d] $E_{v,m=1}$ | [e] $\Gamma_{\Delta v=-2}$ |
|---|---|---|---|---|---|
| 1 | 0.317 | 1.73(-3) | -- | -- | -- |
| 2 | 0.586 | 3.46(-3) | 8.90(-6) | 0.351 | 1.17(-5) |
| 3 | 0.855 | 5.20(-3) | 3.50(-5) | 0.620 | 2.67(-5) |
| 4 | 1.125 | 6.93(-3) | 7.00(-5) | 0.890 | 5.34(-5) |
| 5 | 1.394 | 8.66(-3) | 1.17(-4) | 1.159 | 8.90(-5) |
| 6 | 1.664 | 1.04(-2) | 1.75(-4) | 1.428 | 1.33(-4) |

[a] $E_{v,m=2} = -0.0873+0.269(v+1/2)$
[b] $\Gamma_{\Delta v=-1} = 1.73(-3)v$
[c] $\Gamma_{\Delta v=-2} = 5.83(-6)v(v-1)$
[d] $E_{v,m=1} = -0.322+0.269(v+1/2)$
[e] $\Gamma_{\Delta v=-2} = 4.45(-6)v(v-1)$

An important aspect of the present scattering path hamiltonian is the presence of the linear term in the potential V'(r,t) (cf. Equation 36.). This gave rise to the important $\Delta v = -1$ resonances. In contrast the reaction path hamiltonian does not contain linear terms in the potential and so $\Delta v = -1$ transitions (within the DWBA) would arise only from curvature terms in the kinetic energy operator(42,43). (Thus, a zero-curvature reaction path hamiltonian would not produce $\Delta v = -1$ resonances.) For this reason and for its simplicity, the use of a scattering path hamiltonian should be considered along with the reaction path hamiltonian for addition reactions. Skodje et al. recently reported DWBA calculations of resonance energies and widths for several collinear reactive scattering systems using a vibrationally adiabatic model based on a reaction path hamiltonian(45).

## Summary and prognosis

We have presented a sample of resonance phenomena and calculations in reactive and non-reactive three-body systems. In all cases a two-mathematical dimensional dynamical space was considered, leading to a great simplification in the computational effort. For the H+CO system, low-energy coupled-channel calculations are planned in the future to test the reliablity of the approximations used here, i.e., the scattering path hamiltonian as well as the distorted wave Born approximation. Hopefully these approximations will prove useful in larger systems where coupled-channel calculations would be prohibitively difficult to do. Such approximations will be necessary as resonance phenomena will continue to attract the attention of experimentalists and theorists for many years.

Acknowledgments: The work at IIT was supported in part by the National Science Foundation (CHE-811784) (the complex coordinate calculations) and the U. S. Department of Energy, Office of Basic Energy Sciences (DE-AC02-81ER10900) (the $H+H_2$ resonances). The work at Argonne National Laboratory was supported by the U. S. Department of Energy, Division of Chemical Sciences under contract W-31-109-Eng-38.

## Literature Cited

1. Christoffel, K. M.; Bowman, J. M. J. Chem. Phys. 1983, 78, 3952.
2. Bowman, J. M.; Ju, G.-Z.; Lee, K.-T. J. Chem. Phys. 1981,75, 5199.
3. Bowman, J. M.; Ju, G.-Z.; Lee, K.-T. J. Phys. Chem. 1982, 86, 2232.
4. Bowman, J. M.; Lee, K.-T. Chem. Phys. Lett. 1983, 74, 363.
5. Bowman, J. M.; Lee, K.-T.; Walker, R. B. J. Chem. Phys. 1983, 79, 3742.
6. Lee, K.-T.; Bowman, J. M.; Wagner, A. F.; Schatz, G. C. J. Chem. Phys. 1982, 76, 3583.
7. Bowman, J. M.; Wagner, A. F.; Walch, S. P.; Dunning, Jr., T. H. "Reaction dynamics for $O(^3P)+H_2$ $D_2$. IV. Reduced dimensionality quantum and quasiclassical rate constants with an adiabatic incorporation of the bending motion", J. Chem. Phys., accepted for publication.
8. Bowman, J. M.; Lee, K.-T.; Ju, G.-Z. Chem. Phys. Lett. 1982, 86, 384.
9. Lee, K.-T.; Bowman, J. M. J. Phys. Chem. 1982, 86, 2289.
10. Bowman, J. M. "Reduced dimensionality quantum theories of reactive scattering", Adv. Chem. Phys., to be published.
11. Schatz, G. C.; Kuppermann, A. J. Chem. Phys. 1976, 65, 4642, 4668.
12. Curtiss, C. F.; Hirschfelder, J. O.; Adler, F. T. J. Chem. Phys. 1950, 18, 1638.
13. Pack, R. T J. Chem. Phys. 1974, 60, 633.
14. Kuppermann, A.; Schatz, G. C.; Dwyer, J. P. Chem. Phys. Lett. 1977, 45, 71.
15. See, for example, Townes, C. H.; Schalow, A. L. "Microwave Spectroscopy", McGraw-Hill: New York, 1955, Chapt. 3.

16. Walker, R. B.; Hayes, E. F. J. Phys. Chem. 1983, 87, 1255.
17. Hayes, E. F.; Walker, R. B. "Reactive differential cross sections in the rotating linear model: reactions of fluorine atoms with hydrogen molecules and their isotopic variants", J. Phys. Chem., submitted
18. Walker, R. B.; Blais, N. C.; Truhlar, D. G. J. Chem. Phys. 1984, 84, 246.
19. Porter, R. N.; Karplus, M. J. Chem. Phys. 1964, 40, 1105.
20. Schatz, G. C.; Kuppermann, A. Phys. Rev. Lett. 1975, 35, 1266.
21. Redmon, M. J.; Wyatt, R. E. Chem. Phys. Lett. 1979, 63, 209.
22. Eastes, W.; Marcus, R. A. J. Chem. Phys., 1973, 59, 4757.
23. Secrest, D.; Johnson, B. R. J. Chem. Phys., 1966, 45, 4556.
24. Secrest, D.; Eastes, W. J. Chem. Phys. 1972, 56, 2502.
25. Heller, E. J. Chem. Phys. Lett. 1973, 23, 102.
26. Numrich, R. W.; Kay, K. G. J. Chem. Phys. 1979, 70, 4343.
27. Truhlar, D. G.; Schwenke, D. W. Chem. Phys. Lett. 1983, 95, 83.
28. For a review, see Beswick, J. A.; Jortner, J. Adv. Chem. Phys. 1981, 47, part 1, 363.
29. Beswick, J. A.; Jortner, J. J. Chem. Phys. 1978, 68, 2277.
30. Rosen, N. J. Chem. Phys. 1933, 1, 319.
31. Cooley, J. W. Math. Comput. 1961, 15, 363.
32. We thank Professor C. W. McCurdy for a copy of his Cooley-Numerov code.
33. Beswick, J. A.; Jortner, J. J. Chem. Phys. 1978, 69, 512.
34. Langhoff, S. R.; Davidson, E. R. Int. J. Quant. Chem. 1974, 8, 61.
35. Davidson, E. R.; Silver, D. W. Chem. Phys. Lett. 1978, 52, 403.
36. Dunning, Jr.; T. H., Hay, P. J. "Methods of Electronic Structure Theory", Schaefer, III, H. F., Ed.; Plenum: New York, 1971, Chapt. 1.
37. Dunning, Jr., T. H. J. Chem. Phys. 1980, 73, 2304.
38. Simons, G.; Parr, R. G.; Finlan, J. M. J. Chem. Phys. 1973, 59, 3229.
39. Simons, G. J. Chem. Phys. 1974, 61, 369.
40. Wang, H. Y.; Eyre, J. A.; Dorfman, L. M. J. Chem. Phys. 1973, 59, 5199.
41. Warneck, P. Z. Naturforsch. Teil A 1974, 29, 350.
42. Marcus, R. A. J. Chem. Phys. 1968, 49, 2610 and references therein.
43. Miller, W. H.; Handy, N. C.; Adams, J. E. J. Chem. Phys. 1980, 72, 99.
44. Geiger, L. C.; Schatz, G. C.; Garrett, B. C. "Resonances in the collisional excitation of CO by fast H atoms", this volume.

RECEIVED June 11, 1984